Abiotic versus biotic controls on soil nitrogen cycling in drylands along a 3200-km transect

Dongwei Liu[1]*, Weixing Zhu[1, 2], Xiaobo Wang[1]*, Yuepeng Pan[3], Chao Wang[1], Dan Xi[1], Edith Bai[1], Yuesi Wang[3], Xingguo Han[1], Yunting Fang[1, 4]

[1]Key Laboratory of Forest Ecology and Management, Institute of Applied Ecology, Chinese Academy of Sciences, Shenyang, 110016, China

[2]Department of Biological Sciences, Binghamton University-State University of New York, Binghamton, NY 13902

[3]State Key Laboratory of Atmospheric Boundary Layer Physics and Atmospheric Chemistry (LAPC), Institute of Atmospheric Physics, Chinese Academy of Sciences, Beijing, 100029, China

[4]Qingyuan Forest CERN, Chinese Academy of Sciences, Shenyang 110016, China

*These authors contributed equally to this work.

Corresponding Author:

Weixing Zhu

Department of Biological Sciences, Binghamton University-State University of New York, Binghamton, NY 13902-6000

Phone: (607)-777-3218

Fax: (607)-777-6521

Email: wxzhu@binghamton.edu

Yunting Fang

Institute of Applied Ecology, the Chinese Academy of Science, No.72, Wenhua Road, Shenyang, P. R. China, 110016

Phone: +86-24-83970541

Fax: +86-24-83970300

Email: fangyt@iae.ac.cn

Abstract

Nitrogen (N) cycling in drylands under changing climate is not well understood. Our understanding of N cycling over larger scales to date relies heavily on the measurement of bulk soil N, and the information about internal soil N transformations remains limited. The ^{15}N natural abundance ($\delta^{15}N$) of ammonium and nitrate can serve as a proxy record for the N processes in soils. To better understand the patterns and mechanisms of N cycling in drylands, we collected soils along a 3200-km transect at about 100-km intervals in northern China, with mean annual precipitation (MAP) ranging from 36 mm to 436 mm. We analyzed N pools and $\delta^{15}N$ of ammonium, dual isotopes (^{15}N and ^{18}O) of nitrate, and the microbial gene abundance associated with soil N transformations. We found that N status and its driving factors were different above and below a MAP threshold of 100 mm. In the arid zone with MAP below 100 mm, soil inorganic N accumulated, with a large fraction being of atmospheric origin and ammonia volatilization was strong in soils with high pH. In addition, the abundance of microbial genes associated with soil N transformations was low. In the semiarid zone with MAP above 100 mm, soil inorganic N concentrations were low and controlled mainly by biological processes (e.g., plant uptake and denitrification). The preference for soil ammonium over nitrate by the dominant plant species may enhance the possibility of soil nitrate losses *via* denitrification. Overall, our study suggests that a shift from abiotic to biotic controls on soil N biogeochemistry under global climate changes would greatly affect N losses, soil N availability, and other N transformation processes in these drylands in China.

Key words: soil inorganic N; ^{15}N natural abundance; soil microorganisms; functional genes; spatial patterns

1 Introduction

Drylands cover approximately 41% of the Earth's land surface and play an essential role in providing ecosystem services and regulating carbon (C) and nitrogen (N) cycling (Hartley et al., 2007; Poulter et al., 2014; Reynolds et al., 2007). After water, N availability is the most important limiting factor for plant productivity and microbial processes in dryland ecosystems (Collins et al., 2008; Hooper and Johnson, 1999). Despite low soil N mineralization rates, N losses are postulated to be higher relative to N pools in dryland ecosystems compared with mesic ecosystems (Austin, 2011; Austin et al., 2004; Dijkstra et al., 2012). However, we still lack a full understanding of the constraints on N losses in drylands because multiple processes contribute to N losses, and the response of those processes to changing climate is highly variable (Nielsen and Ball, 2015). The precipitation regimes in drylands are predicted to change during the 21st century (IPCC, 2013), and more extreme climatic regimes will make dryland ecosystems more vulnerable to enhanced drought in some regions and intensive rain in others (Huntington, 2006; Knapp et al., 2008). Therefore, improving our understanding of N cycling and its controls would greatly enhance our ability to predict the responses of dryland ecosystems to global changes.

The natural abundance of ^{15}N (expressed as $\delta^{15}N$) provides critical information on N cycling and thus assists in understanding ecosystem N dynamics over large scales (Amundson et al., 2003; Austin and Vitousek, 1998; Houlton et al., 2006). The general pattern that foliar and soil $\delta^{15}N$ increases as precipitation decreases has been observed at both the regional

(Aranibar et al., 2004; Austin and Vitousek, 1998; Cheng et al., 2009; Peri et al., 2012) and global scales (Amundson et al., 2003; Craine et al., 2009; Handley et al., 1999), suggesting that N cycling is more open (i.e., greater input and output relative to internal cycling) in dryland ecosystems compared with mesic ecosystems. The underlying explanation is that in drylands N supply is higher than biotic demand, resulting in proportionally more N loss through leaching and gaseous N emission relative to the internal N pool (Austin and Vitousek, 1998). Given that the isotope fractionation during N loss is against the heavier isotope, soils and plant tissues become enriched in ^{15}N with increasing N losses (Robinson, 2001). However, the effects of atmospheric deposition on N cycling are often ignored in N isotope studies, in which N isotopes derived from atmospheric deposition and biological N fixation are assumed to be uniform over large regional scales (Bai et al., 2012; Handley et al., 1999; Houlton and Bai, 2009). In addition, N losses in dryland ecosystems are likely dominated by gaseous losses (McCalley and Sparks, 2009; Peterjohn and Schlesinger, 1990). The natural abundance of ^{15}N in soil total N is limited in its usefulness in interpreting the specific processes governing gaseous N losses. Therefore, it seems that the measurement of total N alone is not sufficient to reveal the responses of N cycling to changing precipitation, because there are multiple processes that contribute to the $\delta^{15}N$ variability in plant-soil systems.

Ammonium (NH_4^+) and nitrate (NO_3^-) isotopes can serve as a proxy record for N processes in soils because they directly respond to the *in situ* processes that control production and consumption of NH_4^+ and NO_3^-. For example, comparing $\delta^{15}N$ values of NH_4^+, NO_3^-, and bulk soil N could reveal the relative importance of N transformation processes (such as between ammonification and nitrification) (Koba et al., 2010; Koba et al., 1998). Dual isotope analysis of NO_3^- (^{15}N and ^{18}O of soil NO_3^-) provides evidence for microbial denitrification in oceans (Sigman et al., 2009), forests (Fang et al., 2015; Houlton et al., 2006; Wexler et al., 2014) and groundwater (Minet et al., 2012). In addition, the $\delta^{18}O$ in NO_3^- has been used to partition microbially produced NO_3^- from atmospheric sources because microbial and atmospheric sources cover a different range of $\delta^{18}O$ (Böhlke et al., 1997; Brookshire et al., 2012; Kendall et al., 2007). The positive correlations between N isotopes of available soil N (NH_4^+, NO_3^-, and dissolved organic N) and plant leaves have been used to study the preferences of plant N uptake (Cheng et al., 2010; Houlton et al., 2007; Mayor et al., 2012; Takebayashi et al., 2010). With newly developed methods (Lachouani et al., 2010; Liu et al., 2014; Tu et al., 2016), the analysis of isotopic values in soil NH_4^+ and NO_3^- has the potential to elucidate the N cycling characteristics and their controls; however, compared with the $\delta^{15}N$ of bulk soil N, the $\delta^{15}N$ of soil NH_4^+ and NO_3^- has rarely been reported, especially in drylands.

Soil microbes constitute a major portion of the biota in terrestrial ecosystems and play key roles in regulating ecosystem functions and biogeochemical cycles (van Der Heijden et al., 2008). Linking soil microbial communities and N processes is critical for evaluating the response of N transformations to climate changes. However, despite the rapid development of high-throughput sequencing techniques in recent decades, there is still a great challenge for researchers to establish such linkages due to technical limitations, especially at large spatial scales (Zhou et al., 2011). Alternatively, a microarray-based metagenomics technology, GeoChip, has been developed for the analysis of microbial communities (He et al., 2007; He et al., 2010b; Tu et al., 2014). This technique can be used not only to analyze the functional diversity, composition and structure of microbial communities but also to directly reveal the linkages between microbial communities and ecosystem functions (He

et al., 2007). Functional gene microarray approaches have been used to examine the response of microbially mediated N processes under different environmental conditions. Denitrification genes from the soils in Antarctica, for example, are associated with increased soil temperatures, and N_2-fixation genes are associated with the presence of lichens (Yergeau et al., 2007). Research along an elevation gradient in the Tibetan grassland noted that some denitrification genes (*nir*S and *nos*Z) are more abundant at higher elevations, with nitrification as the major process of nitrous oxides (N_2O) emission (Yang et al., 2013). The latest version, GeoChip 5.0S, contains probes covering more than 144, 000 functional genes, which enables us to explore key microbially mediated biogeochemical processes more thoroughly than ever before (Cong et al., 2015; Wang et al., 2014).

In this study, we studied the effects of water availability on ecosystem-level N availability and cycling along a 3200-km transect in northern China. This natural gradient of precipitation provides an ideal system for identifying the response of soil N dynamics to water availability. In a previous study we reported a hump-shaped pattern of $\delta^{15}N$ in bulk soil N along this precipitation gradient, with a threshold at an aridity index of 0.32 (mean annual precipitation of approximately 250 mm), demonstrating the respective *soil microbial vs. plant* controls (Wang et al., 2014). Here, we further analyzed the concentrations and N isotopic compositions of soil NH_4^+ and NO_3^- (as well as oxygen (O) isotopes for NO_3^-) and the abundance of microbial genes associated with soil N transformation. The principal objectives of this study were to examine (1) the patterns of concentrations and $\delta^{15}N$ values for soil NH_4^+ and NO_3^-; (2) the patterns of gene abundance associated with microbially regulated soil processes; and (3) the responses of soil N cycling to changes in water availability along the precipitation gradient in dryland ecosystems.

2 Materials and methods

2.1 Study areas

The research was carried out along a 3200-km transect across Gansu Province and Inner Mongolia in northern China, covering a longitude from 87.4ºE to 120.5ºE and a latitude from 39.9ºN to 50.1ºN (Fig. 1). The climate is predominantly arid and semi-arid continental. From west to east along the transect, the mean annual precipitation (MAP) increases from 36 mm to 436 mm, the mean annual temperature (MAT) decreases from 9.9 ºC to -1.8 ºC (Fig. S1), and the aridity index (the ratio of precipitation to potential evapotranspiration) ranges from 0.04 to 0.60 (Fig. S1). Vegetation types distributed along the transect were mainly desert, desert steppe, typical steppe and meadow steppe; the three dominant grass genera were *Stipa* spp., *Leymus* spp., and *Cleistogenes* spp., and the three shrub genera were *Nitraria* spp., *Reaumuria* spp., and *Salsola* spp.. Soil types from west to east along the transect are predominantly arid, sandy, and calcium-rich brown loess.

2.2 Soil sampling and sample preparation

Soil sampling was conducted from July to August 2012, the peak of the plant growing season. This is the same transect as described in Wang et al. (2014), but with slightly different site coverage. We selected 36 sites at approximately 100-km intervals between adjacent sites due to limited time to extract soil with KCl solution on the same day after intensive sampling

(Fig. 1), whereas 50 sites at approximately 50-km intervals were used for bulk soil N isotopes measurement in Wang et al. (2014). At each site, we set a 50 m × 50 m plot and five 1 m × 1 m subplots at the four corners and the center of the plot. In each subplot, twenty mineral soil samples were randomly collected using soil cores (2.5 cm diameter × 10 cm depth) and were then thoroughly mixed into one composite sample. The fresh soils were sieved (2 mm) to remove roots and rocks, homogenized by hand and separated into three portions. The first portion was extracted in 2 M KCl (1:5 w/v) for 1 h on the same sampling day; the extracts were stored at 4 ºC during the sampling trip. The second portion was placed in a sterile plastic bag and immediately stored at -40 ºC for later DNA extraction. The third portion was placed in a plastic bag and stored in a refrigerator at 4 ºC for subsequent analyses.

2.3 Analyses of soil physicochemical properties and isotopes

Soil pH was measured using a pH meter and a soil to water ratio of 1:2.5. Soil N content and natural abundance of ^{15}N were determined by an elemental analyzer connected to an Isotope Ratio Mass Spectrometer (IRMS) (Wang et al., 2014). The concentrations of soil NH_4^+ and NO_3^- in the KCl extracts were analyzed using conventional colorimetric methods (Liu et al., 1996). Ammonium concentrations were determined using the indophenol blue method, and nitrate concentrations were determined using the sulfanilamide-NAD reaction following cadmium (Cd) reduction.

The analyses of the isotope compositions of NH_4^+ and NO_3^-, including $\delta^{15}N$ of NH_4^+, $\delta^{15}N$ of NO_3^-, and $\delta^{18}O$ of NO_3^- ($\delta = [(R_{sample}/ R_{standard}) - 1] \times 1000$, where R denotes the ratio of the heavy isotope to the light isotope for N or O, in units per mil, ‰), were based on the isotopic analysis of N_2O. Specifically, NH_4^+ in the extract was oxidized to NO_2^- by alkaline hypobromite (BrO^-) and then reduced to N_2O by hydroxylamine (NH_2OH) (Liu et al., 2014). Nitrate was firstly reduced to NO_2^- by Cd power and then to N_2O by sodium azide (NaN_3) in an acetic acid buffer (McIlvin and Altabet, 2005; Tu et al., 2016). To correct for machine drift and to blank over the isotopic analyses, international standards of NH_4^+ (IAEA N1, USGS 25, and USGS 26) and NO_3^- (IAEA N3, USGS 32, USGS 34, and USGS 35) were treated in identical analytical procedures as the samples to obtain a calibration curve between the measured and expected isotope values. The isotopic signatures of the produced N_2O were determined by an IsoPrime 100 continuous flow isotope ratio mass spectrometer connected to a Trace Gas (TG) pre-concentrator (Liu et al., 2014). The analytical precision for isotopic analyses was better than 0.3‰ (n = 5).

2.4 DNA extraction and GeoChip analysis

For soil DNA extraction, purification, and quantification and the analysis of functional structure of soil microbial communities, we adopted the same approaches as described previously (Wang et al., 2014). In addition to the abundance of nitrification and denitrification genes reported in Wang et al. (2014), the abundance of N fixation, ammonification, and anaerobic ammonia oxidation (anammox) genes was included in this paper. Briefly, microbial genomic DNA was extracted from 0.5 g soil using the MoBioPowerSoil DNA isolation kit (MoBio Laboratories, Carlsbad, CA, USA) and purified by agarose gel electrophoresis followed by phenol-chloroform-butanol extraction. DNA quality was assessed by the A260/280 and A260/230 ratios using a NanoDrop ND-1000 Spectrophotometer (NanoDrop Technologies Inc., Wilmington, DE), and final soil DNA concentrations

were quantified with PicoGreen using a FLUOstar Optima (BMG Labtech, Jena, Germany). The GeoChip 5.0S, manufactured by Agilent (Agilent Technologies Inc., Santa Clara, CA), was used for analyzing DNA samples. The experiments were conducted as described previously (Wang et al., 2014). In brief, the purified DNA samples (0.6 μg) were used for hybridization, and were labeled with the fluorescent dye Cy 3. Subsequently, the labeled DNA was resuspended and hybridized at 67 ºC in an Agilent hybridization oven for 24 h. After washing and drying, the slides were scanned by a NimbleGen MS200 scanner (Roche, Madison, WI, USA) at 633 nm using a laser power of 100% and a photomultiplier tube gain of 75%. The image data were extracted using the Agilent Feature Extraction program (Agilent Technologies, Santa Clara, CA, USA). The raw microarray data were further processed for subsequent analysis using an in-house pipeline that was built on a platform at the Institute for Environmental Genomics, University of Oklahoma (He et al., 2010a; He et al., 2007).

2.5 Statistical analyses

All analyses were conducted using the software package SPSS 18.0 (SPSS, Chicago, IL) for Windows. Pearson correlation analysis was conducted to examine the linear relationships between different variables. Independent-samples T-tests were performed to examine the differences in the investigated variables between arid zone soils and semiarid zone soils. Statistically significant differences were set at a *P*-value of 0.05 unless otherwise stated.

3 Results

3.1 Soil NO_3^- and NH_4^+ concentrations

We found significant inorganic N accumulation in the investigated soil layer (0-10 cm) in sites with a MAP less than 100 mm ($P < 0.01$; Figs. 2b and c). Furthermore, the abundance of microbial genes associated with soil N transformations was significantly reduced compared with that in sites with a MAP greater than 100 mm (see below). Together with the vegetation distribution along the transect (Fig. 1), these results indicated that soil N status and its controls could be different above and below a MAP threshold of 100 mm. Therefore, we hereafter refer to the areas with MAP from 36 mm to 102 mm (15 sites) and from 142 mm to 436 mm (21 sites) as arid zone and semiarid zone, respectively.

In the arid zone, soil NO_3^- concentrations were highly variable and reached up to 1400 mg N kg^{-1}, with a mean of 87 mg N kg^{-1}. Ammonium concentrations varied from 2.0 to 9.9 mg N kg^{-1}, with a mean of 4.3 mg N kg^{-1}. In the semiarid zone, NO_3^- and NH_4^+ concentrations were low -less than 5 mg N kg^{-1} in most samples. Soil NH_4^+ concentrations exhibited a quadratic relationship with increasing MAP in the semiarid zone, but NO_3^- concentrations remained low and did not change with increasing MAP. As expected, bulk soil N was significantly greater in the semiarid zone (on average 0.1%) compared with the arid zone (on average 0.02%) and increased dramatically in the semiarid zone with increasing precipitation (Fig. 2a). Our results suggest increased inorganic N availability in the arid zone compared with the semiarid zone despite a smaller total N pool, which supports the idea that N availability is greater in dry areas compared with less dry areas.

3.2 The ^{15}N natural abundance of soil NO_3^- and NH_4^+

The $\delta^{15}N$ values for NO_3^- were significantly greater in the semiarid zone (0.5 to 19.2‰) compared with the arid zone (-1.2 to 23.4‰; $P < 0.01$; Fig. 2f), with means of 8.4‰ and 6.3‰, respectively. With increasing MAP, the $\delta^{15}N$ value for NO_3^- increased in the arid zone but decreased in the semiarid zone, suggesting different controlling factors in areas with different water availability. Unlike the $\delta^{15}N$ for soil NO_3^-, the $\delta^{15}N$ value for NH_4^+ was significantly greater in the arid zone (-1.2 to 20.2‰) compared with the semiarid zone (-13.9 to 12.6‰; $P < 0.01$; Fig. 2e), with means of 9.2‰ and -0.3‰, respectively. The $\delta^{15}N$ of NH_4^+ was negatively correlated with the MAP in the semiarid zone but was stable as precipitation increased in the arid zone (Fig. 2e).

The N isotopic signature of NH_4^+ and NO_3^- reflects not only the isotopic fractionation during N transformation processes, but also the N isotopic signature of their main sources (i.e., bulk soil N and NH_4^+, respectively). Therefore, we also calculated the relative ^{15}N enrichment of soil NH_4^+ (the difference between the $\delta^{15}N$ of NH_4^+ and bulk soil N) and NO_3^- (the difference between the $\delta^{15}N$ of NO_3^- and NH_4^+) to examine the isotopic imprint of N transformations on soil NH_4^+ and NO_3^-. The relative ^{15}N enrichment of soil NH_4^+ in the arid zone was mostly above zero, whereas its value was below zero in the semiarid zone (Fig. 3a). A negative correlation was observed between MAP and the relative ^{15}N enrichment of soil NH_4^+ across both the arid and semiarid zones (Fig. 3a). According to the Rayleigh model, sinks are always ^{15}N-depleted relative to their sources (Robinson, 2001). The positive values for the relative ^{15}N enrichment of NH_4^+ support the notion that net NH_4^+ losses occurred mainly in the arid zone, whereas the negative values imply that net NH_4^+ gain (e.g., via microbial N mineralization, biological N fixation and/or N deposition) might increase in the semiarid zone, and subsequently reduce the relative ^{15}N enrichment of soil NH_4^+. In a similar manner, we found that the relative ^{15}N enrichment of NO_3^- was mostly below zero in the arid zone and above zero in the semiarid zone (Fig. 3b). A positive correlation was observed between the MAP and the relative ^{15}N enrichment of soil NO_3^- in both the arid and semiarid zone (Fig. 3b). Accordingly, these results suggest that NO_3^- losses increase when water becomes more available, and the residual soil NO_3^- becomes progressively enriched in ^{15}N.

3.3 The abundance of microbial functional genes

The abundances of microbial genes of five main N cycling groups (N fixation, ammonification, nitrification, denitrification, and anammox) were measured at all sites. In arid zone soils, the abundances of all N cycling genes were extremely low (Fig .4), indicating limited microbial potential in this very dry environment. A sharp increase (by 8- to 9-fold) in the gene abundance was noted from the arid zone to the semiarid zone (Fig. 4), even though the soils were still mostly dry at the time of sampling (see soil moisture in Fig. S2). The gene abundances in the semiarid zone were 1 to 2 orders of magnitude greater than those in the arid zone. In addition, the microbial gene abundances of the five main N cycling groups all increased with increasing precipitation in both the arid and semiarid zones (Fig. 4), suggesting a potential effect of water availability on soil microbial N processes.

4 Discussion

4.1 Losses of soil NO_3^- and NH_4^+

We observed different patterns of N cycling above and below a MAP threshold of 100 mm along this 3200-km transect. In the semiarid zone, the increased precipitation seemed to lead to increased losses of soil NO_3^-, but not NH_4^+ (Fig. 3). Soil NO_3^- can be removed from the ecosystem via denitrification, leaching, and plant and microbial uptake. The close correlation between the measured dual isotopes ($\delta^{15}N$ and $\delta^{18}O$) of soil NO_3^- suggests the occurrence of denitrification in the semiarid zone. Microbial denitrification exerts large fractionation against the isotopically heavier compounds, ranging between 5 and 25‰ for both O and N in NO_3^- (Granger et al., 2008). This type of fractionation results in concurrent increases in the $\delta^{18}O$ and $\delta^{15}N$ values of the remaining NO_3^- with a ratio of 0.5 to 1 (Kendall et al., 2007). In the present study, the $\delta^{18}O$ values of soil NO_3^- were significantly correlated with the $\delta^{15}N$ values of soil NO_3^- in the semiarid zone, with a slope of 0.7 (Fig. 5b). This slope is very similar to the slope of 0.8 observed in soil NO_3^- across five Hawaiian tropical forests (Houlton et al., 2006), indicating the occurrence of denitrification-driven NO_3^- losses. Denitrification is regulated by proximal factors, such as NO_3^- concentration and O_2 concentration that immediately affect denitrifying communities (Saggar et al., 2013). Nitrate can be supplied through enhanced microbial processes, including nitrification, when water becomes more available. Increased soil respiration in hot spots and/or hot moments caused by pulse precipitation consumes O_2, consequently favoring denitrification (Abed et al., 2013). In the semiarid zone, we observed that the relative ^{15}N enrichment of soil NO_3^- increased with increasing precipitation (Fig. 3b), suggesting that denitrification may become more favorable with increasing precipitation. In addition, in our preliminary study, a ^{15}N-labeled NO_3^- incubation experiment revealed that potential N_2 losses via denitrification also increased with increasing precipitation in the semiarid soils (Liu and Fang, unpublished data). Because gaseous N losses occur during both nitrification (see below) and denitrification, the coupled nitrification and denitrification could maintain low soil NO_3^- concentrations while enriching the ^{15}N signal of soil NO_3^-.

In the arid zone, the $\delta^{15}N$ and the relative ^{15}N enrichment of soil NO_3^- both increased with increasing precipitation (Figs. 2f and 3b), indicating that denitrification may also occur. However, in these arid soils, microbial gene abundances were considerably lower (Fig. 4), suggesting limited biological activities. It is therefore more likely that microbial denitrification is only a minor process in arid zone soils and may only occur after a large rain event. Microbial denitrification has been observed in hotspots after heavy precipitation events in some desert soils (Abed et al., 2013; Zaady et al., 2013). Alternatively, chemodenitrification may cause soil NO_3^- losses in the arid zone. Chemodenitrification is an abiotic process in which the reduction of NO_2^- to NO and N_2O is coupled to the oxidation of reduced metals (e.g. Fe (II)) and humic substances (Medinets et al., 2015; Zhu-Barker et al., 2015). In a recent review, Heil et al. (2016) discussed several abiotic reactions involving NO_2^-, including the self-decomposition of NO_2^-, reactions of NO_2^- with reduced metals, nitrosation of soil organic matter (SOM) by NO_2^-, and the reaction between NO_2^- and NH_2OH. In this study, ample soil NO_3^- was present in some arid zone soils (Fig. 2c). In addition, our companion work also observed higher available Fe in arid zone soils (Luo et al., 2016). Roco et al. (2016) demonstrated that the first step of denitrification, the dissimilatory reduction of NO_3^- to NO_2^-, was much more common under

aerobic conditions than commonly realized, could occur in diverse bacteria groups and has multiple types of physiological controls. Homyak et al. (2016) reported both initial abiotic NO pulses after soil rewetting and subsequent biologically driven NO emissions, suggesting multiple biotic and abiotic controls on NO emissions and N losses in dryland ecosystems.

In contrast to the $\delta^{15}N$ of soil NO_3^-, the $\delta^{15}N$ values for soil NH_4^+ and their relative ^{15}N enrichment were greater in the arid zone compared with the semiarid zone (Figs. 2e and 3a), suggesting losses of NH_4^+ at the drier sites. We suggest that NH_3 volatilization should play a significant role in NH_4^+ losses because soil pH was higher in the arid zone (from 7.3 to 9.7; Fig. 6a). The isotopic effect of NH_3 volatilization had been reported to be 40 to 60‰ (Robinson, 2001), resulting in ^{15}N-enriched soil NH_4^+. The significant negative correlation between the $\delta^{15}N$ values for NH_4^+ and soil pH in this study (Fig. 6b) supported our interpretation. In addition, despite the low microbial gene abundance, nitrification may be able to occur in the arid zone soils. Although nitrifiers are sensitive to water availability, they can remain active in thin water films, resulting in increased nitrification in dry soils (Sullivan et al., 2012). In the process of nitrification, NO losses occur via a "leaky pipe" mechanism (Firestone and Davidson, 1989). In addition, nitrite (NO_2^-) produced during nitrification can be reduced rapidly to NO via chemodenitrification. The reaction of chemodenitrification forms NO via nitrous acid (HNO_2 (aqueous phase), HONO (gas phase)) decomposition (Medinets et al., 2015). Alternatively, nitrifier denitrification can also serve as a mechanism for NO emission by the reduction of NO_2^- upon the recovery of nitrifiers from drought-induced stress (Heil et al., 2016; Homyak et al., 2016).

In the semiarid zone, NH_3 volatilization should be low due to relatively lower pH compared with the arid zone soils (Fig. 6a). Previous studies have found that water addition did not stimulate NH_3 volatilization (Yahdjian and Sala, 2010), however, a recent study observed the opposite trend in a semiarid subtropical savanna (Soper et al., 2016). The increasing available water in the semiarid zone would also stimulate biological N consumption by plants and microbes. The increased aboveground biomass with increasing MAP suggests an increased net plant N accumulation along this precipitation gradient (Wang et al., 2014). Given that the soil NH_4^+ concentration was greater than that of soil NO_3^- in the semiarid zone ($P < 0.001$), the dominant plant species might adapt to prefer NH_4^+ to NO_3^-. This notion is in accordance with the observed relationship between the $\delta^{15}N$ values of plant leaves (non-N fixing species) and soil NH_4^+ ($R^2 = 0.40$; Fig. 7a), but not soil NO_3^- (Fig. 7b). When we plotted this correlation for each plant species, three dominant species (*Stipa* spp., *Cleistogenes* spp., and *Reaumuria* spp.) all showed significant correlation between foliar $\delta^{15}N$ and soil NH_4^+. Plant nitrogen uptake may also exert a fractionation effect on N sources, but it might be negligible in N-limited areas (Craine et al., 2015). This notion may in part explain a lack of strong ^{15}N enrichment in soil NH_4^+ with increasing precipitation. The consumption of NH_4^+ during nitrification could also increase, as indicated by the microbial gene abundance along the precipitation gradient (Fig. 4). The coupled nitrification and denitrification in the semiarid zone could lead to N loss and the ^{15}N enrichment of residual soil NO_3^-, without significantly changing the NO_3^- concentration. On the other hand, enhanced plant uptake (of both soil NH_4^+ and NO_3^-) would diminish soil inorganic N pools and greatly reduce gaseous N losses through either nitrification (Homyak et al., 2016) or denitrification.

Unexpectedly, we detected high anammox gene abundance in these dryland ecosystems (Fig. 4). Anammox is the microbial reaction between NH_4^+ and NO_2^-, and N_2 is the end product (Thamdrup and Dalsgaard, 2002). Previous studies have

found equal consumption of both soil NH_4^+ and NO_3^- through anammox in N-loaded and water-logged areas (Yang et al., 2014; Zhu et al., 2013). However, the only two studies of anammox in drylands to date failed to confirm its importance (Abed et al., 2013; Strauss et al., 2012). Thus, although anammox possesses a fractionation effect of 23 to 29‰ (Brunner et al., 2013), it is difficult to determine its significance in our study at the present time.

Other abiotic processes have also been reported to contribute to N losses in drylands. High soil surface temperature driven by solar radiation may be responsible for gaseous N losses in dryland ecosystems (Austin, 2011; McCalley and Sparks, 2009, 2008), and affect ^{15}N abundance of soil N. Other non-fractionation processes, such as aeolian deposition and water erosion, might also influence N cycle in dryland ecosystems (Austin, 2011; Hartley et al., 2007).

4.2 Sources of soil NO_3^- and NH_4^+

We observed much higher concentrations of soil NO_3^- in the arid zone (Fig. 2c); on average, they were approximately 20-fold higher than those in the semiarid zone. Nitrate can be formed via microbial nitrification, deposited from N-bearing gaseous (e.g., HNO_3) or dry aerosol NO_3^- (Kendall et al., 2007) or as dissolved nitrate in rainwater or snow. If NO_3^- is formed by nitrification, NO_3^- obtains one O atom from soil O_2 and two O atoms from H_2O (Kendall et al., 2007). The $\delta^{18}O$ value of atmospheric O_2 is relatively stable (23.5‰; we assume that the isotopic composition of O_2 in the atmosphere and soils are the same). The $\delta^{18}O$ value of nitrified NO_3^- depends on the $\delta^{18}O$ value of the local water. The $\delta^{18}O$ values of rainwater taken from the areas closest to the arid zone of our dryland transect (Lanzhou City and its surrounding areas) ranged from -19.1 to 5.2‰ (Chen et al., 2015), yielding corresponding $\delta^{18}O$ values of nitrified NO_3^- ranging from -5.3 to 11.3‰ (Fig. 5a). However, the $\delta^{18}O$ values of soil NO_3^- in the arid zone varied from 5.5 to 51.8‰ (Fig. 5a). This disparity between the calculated and measured $\delta^{18}O$ values provided evidence for the minor importance of nitrification. According to previous studies, the higher $\delta^{18}O$ values of soil NO_3^- we observed in the arid zone have rarely been reported for nitrified NO_3^- (Kendall et al., 2007). For example, an *in situ* study conducted on the forest floor soils found that the $\delta^{18}O$ values of nitrified NO_3^- changed from 3.1 to 10.1‰ (Spoelstra et al., 2007). By comparison, atmospheric origin NO_3^- normally has higher $\delta^{18}O$ values because of the chemical oxidation of NO_3^- precursor NO_x (NO and NO_2) (Fang et al., 2011). Previous research found that the $\delta^{18}O$ values of aerosol NO_3^- ranged from 60 to 111‰ in the Dry Valleys of Antarctica (Savarino et al., 2007). This combined information supports the hypothesis that a sizable fraction of NO_3^- in the surface soils of the arid zone is from atmospheric deposition. Nitrate accumulates on the surface soil when experiencing prolonged droughts, which has also been reported in northern Chile, southern California (Böhlke et al., 1997), and the Turpan-Hami area of northwestern China (Qin et al., 2012). As shown in Fig. 5a, a pronounced trend (green arrow) toward higher $\delta^{18}O$ and lower $\delta^{15}N$ values is obvious for elevated NO_3^- concentrations in the arid zone soils, which might be the result of mixed NO_3^- from both soil nitrification and atmospheric deposition. A similar result was observed in the groundwater of the Saharan Desert (Dietzel et al., 2014). In the arid zone, extreme dryness and high alkalinity (an average pH of 8.3) might limit microbial activities, as suggested by the low gene abundance involving N transformations (Fig. 4), which combined with the lack of leaching, would facilitate the preservation of soil NO_3^-.

In the semiarid zone, the $\delta^{18}O$ values of soil NO_3^- were low (0.9-21.0‰), indicating low atmospheric contribution. The deposited NO_3^- generally experiences postdepositional microbial processes, and the original signature of $\delta^{18}O$ will vanish after biological processes occur (Qin et al., 2012). With increasing MAP, nitrification would progressively provide more NO_3^- with lower $\delta^{18}O$ values. The calculated $\delta^{18}O$ values of NO_3^- from nitrification ranged from 2.5 to 6.5‰ based on the $\delta^{18}O$ of soil H_2O (-8 to -2‰; Shenyang site) (Liu et al., 2010). Both autotrophic and heterotrophic nitrification could generate soil NO_3^-. Heterotrophic nitrification, a process which oxidizes organic N to NO_3^-, bypasses NH_4^+. If this process is important, it would provide an additional explanation for the lack of ^{15}N enrichment in soil NH_4^+ (Fig. 3a). The importance of heterotrophic nitrification has been recognized recently in grasslands (Müller et al., 2014; Müller et al., 2004) and forests (Zhang et al., 2014).

Ammonium accumulation was noted in the arid zone soils and the accumulated NH_4^+ was characterized by increased ^{15}N enrichment (Figs. 2b, e). Ammonium is the dominant species in bulk N deposition in China (Liu et al., 2013). Dry deposition is generally the dominant form of deposition under arid climate (Elliott et al., 2009). The $\delta^{15}N$ values of NH_4^+ and NO_3^- in dry deposition were higher than those in wet deposition (Elliott et al., 2009; Garten, 1996; Heaton et al., 1997) and might contribute to the observed ^{15}N enrichment. Our preliminary study also showed that $\delta^{15}N$ values of aerosol NH_4^+ at one arid site (Dunhuang in Gansu Province, MAP = 46 mm) in northwestern China ranged from 0.35 to 36.9‰, with an average of 16.1‰ (Liu and Fang, unpublished data). Similar results were obtained at a site in Japan (Kawashima and Kurahashi, 2011), where the $\delta^{15}N$ of NH_4^+ in suspended particulate matter ranged from 1.3 to 38.5‰, with an average of 11.6‰. It remains unclear why the $\delta^{15}N$ of NH_4^+ in dry deposition is so positive, but it may result from the isotopic exchange of atmospheric ammonia gas and aerosol NH_4^+, which creates aerosol NH_4^+ enriched in ^{15}N (an isotopic effect of 33‰, (Heaton et al., 1997)). In the drylands, biological N fixation is another important N input (Evans and Ehleringer, 1993). In this study, we speculated that biological N fixation by biological soil crusts (BSCs) could contribute to the soil NH_4^+ pool and soil organic N. We found that with decreasing precipitation, the $\delta^{15}N$ of bulk soil N decreased to close to zero per mil (Fig. 2d), which is the expected $\delta^{15}N$ value for NH_4^+ derived from biological N fixation. BSCs were visually observed during soil sampling in the arid zone. A previous study also reported the potential N-fixing activity and ecological importance of BSCs in soil stability and N availability in the grasslands of Inner Mongolia (Liu et al., 2009).

In the semiarid zone, soil NH_4^+ was depleted in ^{15}N relative to bulk soil N, and their differences in $\delta^{15}N$ increased with increasing MAP, which is likely due to gradually enhanced N mineralization (ammonification) in less dry soils. The increase in precipitation was closely correlated to the microbial gene abundance associated with N transformations (Fig. 4). The $\delta^{15}N$ of bulk soil N was quite stable in the semiarid zone, approximately at 5‰ (Fig. 2d). An increase in N mineralization as precipitation increases would bring in more $^{14}NH_4^+$ and progressively lower the $\delta^{15}N$ of soil NH_4^+ (Fig. 2e). The isotopic effect of N mineralization might also be higher than commonly expected. Our laboratory recently found that ^{15}N fractionation during mineralization was up to 6 to 8‰ in two forest soils in northern China (Zhang et al., 2015). The fractionation during mineralization can even be as high as 20‰ at the enzyme level (Werner and Schmidt 2002). With further increase in water

availability in the semiarid zone, N turnover linking the biological uptake (plant and microbes) and return of N could further enhance soil ammonification, which results in lower $\delta^{15}N$ in soil NH_4^+. In addition, there is also a possibility of dissimilatory nitrate reduction to ammonium (DNRA); however, we did not measure this process in our study. DNRA is even less sensitive to oxygen levels than denitrification and may therefore occur in aerobic soils (Müller et al., 2004), contributing to the availability of soil NH_4^+.

5 Summary

Our study reported the pattern of $\delta^{15}N$ in soil inorganic N (NH_4^+ and NO_3^-) across a precipitation gradient from very arid land to semiarid grassland. Together with the analyses of soil N concentration, soil pH and moisture, and functional gene abundance, the compound-specific $\delta^{15}N$ analyses presented here demonstrate a clear shift of *abiotic vs. biotic* (microbes and plants) controls on N cycling along this 3200-km dryland transect in China.

In the arid zone, characterized by extreme aridity (36 mm < MAP < 100 mm; Fig. 8a), plant cover was sparse, and microbial activity was limited (Figs. 1 and 4). Nitrogen input, mostly in the form of atmospheric deposition, largely accumulated, creating "^{15}N-enriched" inorganic N pools despite a much smaller pool of bulk soil N. The accumulation of inorganic N drives abiotic processes that lead to N losses with strong isotopic fractionation effects on the remaining soil N. The higher pH associated with a lower MAP is likely a dominant driver of NH_3 volatilization, causing ^{15}N enrichment in soil NH_4^+. The very high yet variable accumulation of NO_3^- in soil compared with NH_4^+ suggests limited NO_3^- loss under extreme aridity.

In the semiarid zone (100 mm < MAP < 436 mm; Fig. 8b), controls on N cycling increasingly shift from abiotic to biotic factors. Microbial gene abundances associated with N cycling groups were considerably greater when water became more available (Fig. 4). Increasing N mineralization with increasing MAP was accompanied by reduced NH_3 volatilization due to lower pH, producing soil NH_4^+ pools with lighter N isotopes. Ammonification (N mineralization) both supplies NH_4^+ for plant uptake and favors soil nitrification. Both nitrification and denitrification could lead to N loss and isotopically enrich the remaining soil N. Soil heterogeneity and pulse precipitation events could provide hotspots for these microbial processes, whereas increased plant cover and N uptake could reduce the soil NH_4^+ and NO_3^- pools and minimize overall N losses. The regulation of abiotic vs. biotic controls by precipitation on N cycling and N losses suggests that global climate changes would have a great impact on these dryland ecosystems.

Author contribution

Y. Fang, D. Liu, W. Zhu, and X. Han designed the study; D. Liu, X. Wang, Y. Pan, C. Wang, D. Xi, Y. Wang, and X. Han performed the experiment; D. Liu, W. Zhu, Y. Fang, X. Wang, Y. Pan, C. Wang, D. Xi, E. Bai and Y. Wang analysed the data.

D. Liu, W. Zhu, and Y. Fang wrote the manuscript; X. Wang, Y. Pan, C. Wang, E. Bai, and X. Han contributed to discussion of the results and manuscript preparation.

Acknowledgements

The work was financially supported by the National Key Research and Development Program of China (2016YFA0600802), the Strategic Priority Research Program of the Chinese Academy of Sciences (XDB15020200, XDB15010401 and XDA05100100), the National Natural Science Foundation of China (31370464, 31422009, 41405144, and 31600358), Hundred Talents Program of Chinese Academy of Sciences (No.Y1SRC111J6), and State Key Laboratory of Forest and Soil Ecology (LFSE2015-19). We would like to thank Ying Tu, Haiyan Ren, Shasha Zhang, Feifei Zhu, and Xiaoming Fang for their assistance in field sampling and laboratory analysis, and Shaonan Huang for sharing the unpublished data. We thank all members of the sampling team from the Institute of Applied Ecology, Chinese Academy of Sciences for their assistance during field sampling. We would like to thank Ben Eisenkop and Zhengjie Li for their assistance on the English editing. We also thank reviewers and editor for their helpful comments and constructive suggestions which have greatly improved the quality of this paper.

References

Abed, R. M., Lam, P., Beer, D. d., and Stief, P.: High rates of denitrification and nitrous oxide emission in arid biological soil crusts from the Sultanate of Oman, ISME J., 7, 1862-1875, 2013.

Amundson, R., Austin, A. T., Schuur, E. A. G., Yoo, K., Matzek, V., Kendall, C., Uebersax, A., Brenner, D., and Baisden, W.: Global patterns of the isotopic composition of soil and plant nitrogen, Global Biogeochem. Cy., 17, 1031, doi: 10.1029/2002GB001903, 2003.

Aranibar, J. N., Otter, L., Macko, S. A., Feral, C. J. W., Epstein, H. E., Dowty, P. R., Eckardt, F., Shugart, H. H., and Swap, R. J.: Nitrogen cycling in the soil-plant system along a precipitation gradient in the Kalahari sands, Glob. Change Biol., 10, 359-373, 2004.

Austin, A. T., and Vitousek, P.: Nutrient dynamics on a precipitation gradient in Hawai'i, Oecologia, 113, 519-529, 1998.

Austin, A. T., Yahdjian, L., Stark, J. M., Belnap, J., Porporato, A., Norton, U., Ravetta, D. A., and Schaeffer, S. M.: Water pulses and biogeochemical cycles in arid and semiarid ecosystems, Oecologia, 141, 221-235, 2004.

Austin, A. T.: Has water limited our imagination for aridland biogeochemistry?, Trends Ecol. Evol., 26, 229-235, 2011.

Böhlke, J. K., Ericksen, G. E., and Revesz, K.: Stable isotope evidence for an atmospheric origin of desert nitrate deposits in northern Chile and southern California, USA, Chem. Geol., 136, 135-152, 1997.

Bai, E., Houlton, B., and Wang, Y.: Isotopic identification of nitrogen hotspots across natural terrestrial ecosystems, Biogeosciences, 9, 3287-3304, 2012.

Brookshire, E. N. J., Hedin, L. O., Newbold, J. D., Sigman, D. M., and Jackson, J. K.: Sustained losses of bioavailable nitrogen from montane tropical forests, Nat. Geosci., 5, 123-126, 2012.

Brunner, B., Contreras, S., Lehmann, M. F., Matantseva, O., Rollog, M., Kalvelage, T., Klockgether, G., Lavik, G., Jetten, M. S., and Kartal, B.: Nitrogen isotope effects induced by anammox bacteria, P. Natl. Acad. Sci. USA, 110, 18994-18999, 2013.

Chen, F. L., Zhang, M. J., Ma, Q., Wang, S. J., Li, X. F., and Zhu, X. F.: Stable isotopic characteristics of precipitation in Lanzhou city and its surrounding areas, Northwest China, Environ. Earth Sci., 73, 4671-4680, 2015.

Cheng, S. L., Fang, H. J., Yu, G. R., Zhu, T. H., and Zheng, J. J.: Foliar and soil ^{15}N natural abundances provide field evidence on nitrogen dynamics in temperate and boreal forest ecosystems, Plant Soil, 337, 285-297, 2010.

Cheng, W. X., Chen, Q. S., Xu, Y. Q., Han, X. G., and Li, L. H.: Climate and ecosystem ^{15}N natural abundance along a transect of Inner Mongolian grasslands: Contrasting regional patterns and global patterns, Global Biogeochem. Cy., 23, 11-22, 2009.

Collins, S. L., Sinsabaugh, R. L., Crenshaw, C., Green, L., Porras‐Alfaro, A., Stursova, M., and Zeglin, L. H.: Pulse dynamics and microbial processes in aridland ecosystems, J. Ecol., 96, 413-420, 2008.

Cong, J., Liu, X., Lu, H., Xu, H., Li, Y., Deng, Y., Li, D., and Zhang, Y.: Available nitrogen is the key factor influencing soil microbial functional gene diversity in tropical rainforest, BMC Microbiol., 15, 167, doi: 10.1186/s12866-015-0491-8, 2015.

Craine, J. M., Elmore, A. J., Aidar, M. P., Bustamante, M., Dawson, T. E., Hobbie, E. A., Kahmen, A., Mack, M. C., McLauchlan, K. K., and Michelsen, A.: Global patterns of foliar nitrogen isotopes and their relationships with climate, mycorrhizal fungi, foliar nutrient concentrations, and nitrogen availability, New Phytol., 183, 980-992, 2009.

Craine, J. M., Brookshire, E., Cramer, M. D., Hasselquist, N. J., Koba, K., Marin-Spiotta, E., and Wang, L.: Ecological interpretations of nitrogen isotope ratios of terrestrial plants and soils, Plant Soil, 396, 1-26, 2015.

Dietzel, M., Leis, A., Abdalla, R., Savarino, J., Morin, S., Böttcher, M., and Köhler, S.: ^{17}O excess traces atmospheric nitrate in paleo-groundwater of the Saharan desert, Biogeosciences, 11, 3149-3161, 2014.

Dijkstra, F. A., Augustine, D. J., Brewer, P., and von Fischer, J. C.: Nitrogen cycling and water pulses in semiarid grasslands: are microbial and plant processes temporally asynchronous?, Oecologia, 170, 799-808, 2012.

Elliott, E. M., Kendall, C., Boyer, E. W., Burns, D. A., Lear, G. G., Golden, H. E., Harlin, K., Bytnerowicz, A., Butler, T. J., and Glatz, R.: Dual nitrate isotopes in dry deposition: Utility for partitioning NOx source contributions to landscape nitrogen deposition, J. Geophys. Res., 114, G04020, doi: 10.1029/2008JG000889, 2009.

Evans, R., and Ehleringer, J.: A break in the nitrogen cycle in aridlands? Evidence from $\delta^{15}N$ of soils, Oecologia, 94, 314-317, 1993.

Fang, Y. T., Koba, K., Wang, X. M., Wen, D. Z., Li, J., Takebayashi, Y., Liu, X. Y., and Yoh, M.: Anthropogenic imprints on nitrogen and oxygen isotopic composition of precipitation nitrate in a nitrogen-polluted city in southern China, Atmos. Chem. Phys., 11, 1313-1325, 2011.

Fang, Y. T., Koba, K., Makabe, A., Takahashi, C., Zhu, W. X., Hayashi, T., Hokari, A. A., Urakawa, R., Bai, E., Houlton, B. Z., Xi, D., Zhang, S. S., Matsushita, K., Tu, Y., Liu, D. W., Zhu, F. F., Wang, Z. Y., Zhou, G. Y., Chen, D. X., Makita, T.,

Toda, H., Liu, X. Y., Chen, Q. S., Zhang, D. Q., Li, Y. D., and Yoh, M.: Microbial denitrification dominates nitrate losses from forest ecosystems, P. Natl. Acad. Sci. USA, 112, 1470-1474, 2015.

Firestone, M. K., and Davidson, E. A.: Microbiological basis of NO and N_2O production and consumption in soil, in: Exchange of Trace Gases between Terrestrial Ecosystems and the Atmosphere, edited by: Andreae, M. O., and Schimel, D. S., John Wiley & Sons, New York, USA, 7-21, 1989.

Garten, C. T.: Stable nitrogen isotope ratios in wet and dry nitrate deposition collected with an artificial tree, Tellus B, 48, 60-64, 1996.

Granger, J., Sigman, D. M., Lehmann, M. F., and Tortell, P. D.: Nitrogen and oxygen isotope fractionation during dissimilatory nitrate reduction by denitrifying bacteria, Limnol. Oceanogr., 53, 2533-2545, 2008.

Handley, L., Austin, A., Stewart, G., Robinson, D., Scrimgeour, C., Raven, J., and Schmidt, S.: The ^{15}N natural abundance ($\delta^{15}N$) of ecosystem samples reflects measures of water availability, Funct. Plant Biol., 26, 185-199, 1999.

Hartley, A., Barger, N., Belnap, J., and Okin, G. S.: Dryland ecosystems, in: Nutrient Cycling in Terrestrial Ecosystems, edited by: Marschner, P., and Rengel, Z., Springer Berlin Heidelberg, Germany, 271-307, 2007.

He, Z., Deng, Y., Van Nostrand, J. D., Tu, Q., Xu, M., Hemme, C. L., Li, X., Wu, L., Gentry, T. J., Yin, Y., Liebich, J., Hazen, T. C., and Zhou, J.: GeoChip 3.0 as a high-throughput tool for analyzing microbial community composition, structure and functional activity, ISME J., 4, 1167-1179, 2010a.

He, Z. L., Gentry, T. J., Schadt, C. W., Wu, L. Y., Liebich, J., Chong, S. C., Huang, Z. J., Wu, W. M., Gu, B. H., and Jardine, P.: GeoChip: a comprehensive microarray for investigating biogeochemical, ecological and environmental processes, ISME J., 1, 67-77, 2007.

He, Z. L., Xu, M. Y., Deng, Y., Kang, S. H., Kellogg, L., Wu, L. Y., Van Nostrand, J. D., Hobbie, S. E., Reich, P. B., and Zhou, J. Z.: Metagenomic analysis reveals a marked divergence in the structure of belowground microbial communities at elevated CO_2, Ecol. Lett., 13, 564-575, 2010b.

Heaton, T. H. E., Spiro, B., and Robertson, S. M. C.: Potential canopy influences on the isotopic composition of nitrogen and sulphur in atmospheric deposition, Oecologia, 109, 600-607, 1997.

Heil, J., Vereecken, H., and Brüggemann, N.: A review of chemical reactions of nitrification intermediates and their role in nitrogen cycling and nitrogen trace gas formation in soil, Eur. J. Soil Sci., 67, 23-39, 2016.

Homyak, P. M., Blankinship, J. C., Marchus, K., Lucero, D. M., Sickman, J. O., and Schimel, J. P.: Aridity and plant uptake interact to make dryland soils hotspots for nitric oxide (NO) emissions, P. Natl. Acad. Sci. USA, 113, E2608-2616, 2016.

Hooper, D. U., and Johnson, L.: Nitrogen limitation in dryland ecosystems: responses to geographical and temporal variation in precipitation, Biogeochemistry, 46, 247-293, 1999.

Houlton, B. Z., Sigman, D. M., and Hedin, L. O.: Isotopic evidence for large gaseous nitrogen losses from tropical rainforests, P. Natl. Acad. Sci. USA, 103, 8745-8750, 2006.

Houlton, B. Z., Sigman, D. M., Schuur, E. A., and Hedin, L. O.: A climate-driven switch in plant nitrogen acquisition within tropical forest communities, P. Natl. Acad. Sci. USA, 104, 8902-8906, 2007.

Houlton, B. Z., and Bai, E.: Imprint of denitrifying bacteria on the global terrestrial biosphere, P. Natl. Acad. Sci. USA, 106, 21713-21716, 2009.

Huntington, T. G.: Evidence for intensification of the global water cycle: review and synthesis, J. Hydrol., 319, 83-95, 2006.

IPCC: Climate change 2013: the physical science basis: Working Group I contribution to the Fifth assessment report of the Intergovernmental Panel on Climate Change, Cambridge University Press, 2013.

Kawashima, H., and Kurahashi, T.: Inorganic ion and nitrogen isotopic compositions of atmospheric aerosols at Yurihonjo, Japan: Implications for nitrogen sources, Atmos. Environ., 45, 6309-6316, 2011.

Kendall, C., Elliott, E. M., and Wankel, S. D.: Tracing anthropogenic inputs of nitrogen to ecosystem, in: Stable isotopes in ecology & environmental science, edited by: Michener, R., and Lajtha, K., Blackwell Publishing, USA, 375-449, 2007.

Knapp, A. K., Beier, C., Briske, D. D., Classen, A. T., Luo, Y., Reichstein, M., Smith, M. D., Smith, S. D., Bell, J. E., and Fay, P. A.: Consequences of more extreme precipitation regimes for terrestrial ecosystems, Bioscience, 58, 811-821, 2008.

Koba, K., Tokuchi, N., Yoshioka, T., Hobbie, E. A., and Iwatsubo, G.: Natural abundance of nitrogen-15 in a forest soil, Soil Sci. Soc. Am. J., 62, 778-781, 1998.

Koba, K., Isobe, K., Takebayashi, Y., Fang, Y., Sasaki, Y., Saito, W., Yoh, M., Mo, J., Liu, L., and Lu, X.: $\delta^{15}N$ of soil N and plants in a N‐saturated, subtropical forest of southern China, Rapid Commun. Mass Sp., 24, 2499-2506, 2010.

Lachouani, P., Frank, A. H., and Wanek, W.: A suite of sensitive chemical methods to determine the $\delta^{15}N$ of ammonium, nitrate and total dissolved N in soil extracts, Rapid Commun. Mass Sp., 24, 3615-3623, 2010.

Liu, D. W., Fang, Y. T., Tu, Y., and Pan, Y. P.: Chemical method for nitrogen isotopic analysis of ammonium at natural abundance, Anal. Chem., 86, 3787-3792, 2014.

Liu, G. S., Jiang, N. H., Zhang, L. D., and Liu, Z. L.: Soil physical and chemical analysis and description of soil profiles, China Standard Methods Press, Beijing, 24, 1996.

Liu, H. J., Han, X. G., Li, L. H., Huang, J. H., Liu, H. S., and Li, X.: Grazing density effects on cover, species composition, and nitrogen fixation of biological soil crust in an Inner Mongolia steppe, Rangeland Ecol. Manag., 62, 321-327, 2009.

Liu, J. R., Song, X. F., Yuan, G. F., Sun, X. M., Liu, X., and Wang, S. Q.: Characteristics of $\delta^{18}O$ in precipitation over Eastern Monsoon China and the water vapor sources, Chinese Sci. Bull., 55, 200-211, 2010.

Liu, X., Zhang, Y., Han, W., Tang, A., Shen, J., Cui, Z., Vitousek, P., Erisman, J. W., Goulding, K., Christie, P., Fangmeier, A., and Zhang, F.: Enhanced nitrogen deposition over China, Nature, 494, 459-462, 2013.

Luo, W. T., Sardans, J., Dijkstra, F. A., Peñuelas, J., Lü, X. T., Wu, H. H., Li, M. H., Bai, E., Wang, Z. W., Han, X. G., and Jiang, Y.: Thresholds in decoupled soil-plant elements under changing climatic conditions, Plant Soil, 409, 159-173, 2016.

Müller, C., Stevens, R. J., and Laughlin, R. J.: A ^{15}N tracing model to analyse N transformations in old grassland soil, Soil Biol. Biochem., 36, 619-632, 2004.

Müller, C., Laughlin, R. J., Spott, O., and Rütting, T.: Quantification of N_2O emission pathways via a ^{15}N tracing model, Soil Biol. Biochem., 72, 44-54, 2014.

Mayor, J. R., Schuur, E. A., Mack, M. C., Hollingsworth, T. N., and Bååth, E.: Nitrogen isotope patterns in alaskan black spruce reflect organic nitrogen sources and the activity of ectomycorrhizal fungi, Ecosystems, 15, 819-831, 2012.

McCalley, C. K., and Sparks, J. P.: Controls over nitric oxide and ammonia emissions from Mojave Desert soils, Oecologia, 156, 871-881, 2008.

McCalley, C. K., and Sparks, J. P.: Abiotic gas formation drives nitrogen loss from a desert ecosystem, Science, 326, 837-840, 2009.

McIlvin, M. R., and Altabet, M. A.: Chemical conversion of nitrate and nitrite to nitrous oxide for nitrogen and oxygen isotopic analysis in freshwater and seawater, Anal. Chem., 77, 5589-5595, 2005.

Medinets, S., Skiba, U., Rennenberg, H., and Butterbach-Bahl, K.: A review of soil NO transformation: Associated processes and possible physiological significance on organisms, Soil Biol. Biochem., 80, 92-117, 2015.

Minet, E., Coxon, C., Goodhue, R., Richards, K., Kalin, R., and Meier-Augenstein, W.: Evaluating the utility of ^{15}N and ^{18}O isotope abundance analyses to identify nitrate sources: A soil zone study, Water Res., 46, 3723-3736, 2012.

Nielsen, U. N., and Ball, B. A.: Impacts of altered precipitation regimes on soil communities and biogeochemistry in arid and semi-arid ecosystems, Glob. Change Biol., 21, 1407-1421, 2015.

Peri, P. L., Ladd, B., Pepper, D. A., Bonser, S. P., Laffan, S. W., and Amelung, W.: Carbon ($\delta^{13}C$) and nitrogen ($\delta^{15}N$) stable isotope composition in plant and soil in Southern Patagonia's native forests, Glob. Change Biol., 18, 311-321, 2012.

Peterjohn, W. T., and Schlesinger, W. H.: Nitrogen loss from deserts in the southwestern United States, Biogeochemistry, 10, 67-79, 1990.

Poulter, B., Frank, D., Ciais, P., Myneni, R. B., Andela, N., Bi, J., Broquet, G., Canadell, J. G., Chevallier, F., Liu, Y. Y., Running, S. W., Sitch, S., and van der Werf, G. R.: Contribution of semi-arid ecosystems to interannual variability of the global carbon cycle, Nature, 509, 600-603, 2014.

Qin, Y., Li, Y. H., Bao, H. M., Liu, F., Hou, K. J., Wan, D. F., and Zhang, C.: Massive atmospheric nitrate accumulation in a continental interior desert, northwestern China, Geology, 40, 623-626, 2012.

Reynolds, J. F., Smith, D. M. S., Lambin, E. F., Turner, B., Mortimore, M., Batterbury, S. P., Downing, T. E., Dowlatabadi, H., Fernández, R. J., and Herrick, J. E.: Global desertification: building a science for dryland development, Science, 316, 847-851, 2007.

Robinson, D.: $\delta^{15}N$ as an integrator of the nitrogen cycle, Trends Ecol. Evol., 16, 153-162, 2001.

Roco, C. A., Bergaust, L. L., Shapleigh, J. P., and Yavitt, J. B.: Reduction of nitrate to nitrite by microbes under oxic conditions, Soil Biol. Biochem., 100, 1-8, 2016.

Saggar, S., Jha, N., Deslippe, J., Bolan, N. S., Luo, J., Giltrap, D. L., Kim, D. G., Zaman, M., and Tillman, R. W.: Denitrification and N_2O: N_2 production in temperate grasslands: processes, measurements, modelling and mitigating negative impacts, Sci. Total Environ., 465, 173-195, 2013.

Savarino, J., Kaiser, J., Morin, S., Sigman, D., and Thiemens, M.: Nitrogen and oxygen isotopic constraints on the origin of atmospheric nitrate in coastal Antarctica, Atmos. Chem. Phys., 7, 1925-1945, 2007.

Sigman, D. M., DiFiore, P. J., Hain, M. P., Deutsch, C., Wang, Y., Karl, D. M., Knapp, A. N., Lehmann, M. F., and Pantoja, S.: The dual isotopes of deep nitrate as a constraint on the cycle and budget of oceanic fixed nitrogen, Deep Sea Res. Part I Oceanogr. Res. Pap., 56, 1419-1439, 2009.

Soper, F. M., Boutton, T. W., Groffman, P. M., and Sparks, J. P.: Nitrogen trace gas fluxes from a semiarid subtropical savanna under woody legume encroachment, Global Biogeochem. Cy., 30, 614-628, 2016.

Spoelstra, J., Schiff, S. L., Hazlett, P. W., Jeffries, D. S., and Semkin, R. G.: The isotopic composition of nitrate produced from nitrification in a hardwood forest floor, Geochim. Cosmochim. Ac., 71, 3757-3771, 2007.

Strauss, S. L., Day, T. A., and Garcia-Pichel, F.: Nitrogen cycling in desert biological soil crusts across biogeographic regions in the Southwestern United States, Biogeochemistry, 108, 171-182, 2012.

Sullivan, B. W., Selmants, P. C., and Hart, S. C.: New evidence that high potential nitrification rates occur in soils during dry seasons: Are microbial communities metabolically active during dry seasons?, Soil Biol. Biochem., 53, 28-31, 2012.

Takebayashi, Y., Koba, K., Sasaki, Y., Fang, Y. T., and Yoh, M.: The natural abundance of ^{15}N in plant and soil - available N indicates a shift of main plant N resources to NO_3^- from NH_4^+ along the N leaching gradient, Rapid Commun. Mass Sp., 24, 1001-1008, 2010.

Thamdrup, B., and Dalsgaard, T.: Production of N_2 through anaerobic ammonium oxidation coupled to nitrate reduction in marine sediments, Appl. Environ. Microb., 68, 1312-1318, 2002.

Tu, Q., Yu, H., He, Z., Deng, Y., Wu, L., van Nostrand, J. D., Zhou, A., Voordeckers, J., Lee, Y. J., and Qin, Y.: GeoChip 4: a functional gene - array - based high - throughput environmental technology for microbial community analysis, Mol. Ecol. Resour., 14, 914-928, 2014.

Tu, Y., Fang, Y. T., Liu, D. W., and Pan, Y. P.: Modifications to the azide method for nitrate isotope analysis, Rapid Commun. Mass Sp., 30, 1213-1222, 2016.

van Der Heijden, M. G., Bardgett, R. D., and van Straalen, N. M.: The unseen majority: soil microbes as drivers of plant diversity and productivity in terrestrial ecosystems, Ecol. Lett., 11, 296-310, 2008.

Wang, C., Wang, X. B., Liu, D. W., Wu, H. H., Lü, X. T., Fang, Y. T., Cheng, W. X., Luo, W. T., Jiang, P., and Shi, J.: Aridity threshold in controlling ecosystem nitrogen cycling in arid and semi-arid grasslands, Nat. Commun., 5, 4799, doi: 10.1038/ncomms5799, 2014.

Wexler, S. K., Goodale, C. L., McGuire, K. J., Bailey, S. W., and Groffman, P. M.: Isotopic signals of summer denitrification in a northern hardwood forested catchment, P. Natl. Acad. Sci. USA, 111, 16413-16418, 2014.

Yahdjian, L., and Sala, O. E.: Size of precipitation pulses controls nitrogen transformation and losses in an arid patagonian ecosystem, Ecosystems, 13, 575-585, 2010.

Yang, X. R., Li, H., Nie, S., Su, J. Q., Weng, B., Zhu, G., Yao, H. Y., Gilbert, J. A., and Zhu, Y. G.: The potential contribution of anammox to nitrogen loss from paddy soils in Southern China, Appl. Environ. Microb., 81, 938-947, 2014.

Yang, Y. F., Wu, L. W., Lin, Q. Y., Yuan, M. T., Xu, D. P., Yu, H., Hu, Y. G., Duan, J. C., Li, X. Z., He, Z. L., Xue, K., van Nostrand, J., Wang, S. P., and Zhou, J. Z.: Responses of the functional structure of soil microbial community to livestock grazing in the Tibetan alpine grassland, Global Biogeochem. Cy., 19, 637-648, 2013.

Yergeau, E., Kang, S., He, Z., Zhou, J., and Kowalchuk, G. A.: Functional microarray analysis of nitrogen and carbon cycling genes across an Antarctic latitudinal transect, ISME J., 1, 163-179, 2007.

Zaady, E., Groffman, P. M., Standing, D., and Shachak, M.: High N_2O emissions in dry ecosystems, Eur. J. Soil Biol., 59, 1-7, 2013.

Zhang, J. B., Sun, W. J., Zhong, W. H., and Cai, Z. C.: The substrate is an important factor in controlling the significance of heterotrophic nitrification in acidic forest soils, Soil Biol. Biochem., 76, 143-148, 2014.

Zhang, S. S., Fang, Y. T., and Xi, D.: Adaptation of micro-diffusion method for the analysis of ^{15}N natural abundance of ammonium in samples with small volume, Rapid Commun. Mass Sp., 29, 1297-1306, 2015.

Zhou, J. Z., Wu, L. Y., Deng, Y., Zhi, X. Y., Jiang, Y. H., Tu, Q. C., Xie, J. P., Van Nostrand, J. D., He, Z. L., and Yang, Y. F.: Reproducibility and quantitation of amplicon sequencing-based detection, ISME J., 5, 1303-1313, 2011.

Zhu-Barker, X., Cavazos, A. R., Ostrom, N. E., Horwath, W. R., and Glass, J. B.: The importance of abiotic reactions for nitrous oxide production, Biogeochemistry, 126, 251-267, 2015.

Zhu, G., Wang, S., Wang, W., Wang, Y., Zhou, L., Jiang, B., den Camp, H. J. O., Risgaard-Petersen, N., Schwark, L., and Peng, Y.: Hotspots of anaerobic ammonium oxidation at land-freshwater interfaces, Nat. Geosci., 6, 103-107, 2013.

Figure captions

595

Figure 1. Vegetation types and sampling sites distribution along the transect. Across the 3200-km precipitation gradient in northern China, four typical vegetation types are distributed from west to east, which are desert (a), desert steppe (b), typical steppe (c), and meadow steppe (d). The dominant plant genera change gradually from shrub (*Nitraria* spp., *Reaumuria* spp., and *Salsola* spp.) to perennial grasses (*Stipa* spp., *Leymus* spp., and *Cleistogenes* spp.). Soil types are predominantly arid,
600 sandy, and brown loess rich in calcium from west to east of the transect. A total of 36 soil sampling sites were selected.

Figure 2. Nitrogen concentrations and isotopic composition of bulk soil N, NH_4^+, and NO_3^-. The significant ($P < 0.05$) trends are shown with a regression line (red) and 95% confidence intervals (blue). At each site, n = 5.

605 **Figure 3.** The relative ^{15}N enrichment of soil NH_4^+ and NO_3^-. Data in the figures were calculated as the difference between $\delta^{15}N$ of bulk soil N and NH_4^+, and between $\delta^{15}N$ of soil NH_4^+ and NO_3^-, respectively. The significant ($P < 0.05$) trend is shown with a regression line (red) and 95% confidence intervals (blue). At each site, n = 5.

Figure 4. Changes in the abundance of microbial gene involved in N cycling. Signal intensity was standardized based on both
610 the number of array probes and DNA quantity in a gram of dry soil. Each point is the site-averaged value; results of the abundance of nitrification and denitrification genes have been reported in a previous study (Wang et al., 2014). The significant ($P < 0.05$) trends are shown with a regression line (red) and 95% confidence intervals (blue).

Figure 5. Relationship between $\delta^{18}O$ and $\delta^{15}N$ of soil NO_3^-. The range of $\delta^{18}O$ and $\delta^{15}N$ from atmospheric NO_3^- was based on
615 the limited isotope measurement of precipitation. Black points represent precipitation NO_3^- collected from an urban site in Beijing in the year of 2012, with data derived from Tu et al. (2016). Grey points represent precipitation NO_3^- collected from Qingyuan forest CERN (Chinese Ecosystem Research Network, CERN) in northern China in the year of 2014 (Huang and Fang, unpublished data). The range of $\delta^{15}N$ and $\delta^{18}O$ produced by nitrified NO_3^- are positioned by using the $\delta^{15}N$ of soil NH_4^+ in this study (Fig. 2e), and the estimated $\delta^{18}O$ from soil nitrification based on the 1:2 ratio of soil O_2 and H_2O (see Text),
620 respectively.

Figure 6. Soil pH and the relationship with $\delta^{15}N$ of soil NH_4^+. The different patterns of soil pH was observed above and below the threshold at MAP of about 100 mm; data were derived from Wang et al. (2014). There was a positive correlation between $\delta^{15}N$ of soil NH_4^+ and pH across the transect. The significant ($P < 0.05$) trend is shown with a regression line (red) and 95%
625 confidence intervals (blue). At each site, n = 5.

Figure 7. Relationship between the $\delta^{15}N$ of foliage and $\delta^{15}N$ of soil NH_4^+ and NO_3^-. Data on foliar $\delta^{15}N$ (*Stipa* spp., *Leymus* spp., *Cleistogenes* spp., *Reaumuria* spp., and *Salsola* spp.) were from the previous study of Wang et al. (2014). Almost all dominant plants were found in the area with MAP more than 100 mm (semiarid zone). Data are the site-averaged values. The significant ($P < 0.05$) trend is shown with a regression line (thick) and 95% confidence intervals (thin).

Figure 8. A framework of N biogeochemical cycling in dryland ecosystems in northern China. Width of arrows and size of boxes indicate the relative importance (qualitative interpretation) of soil N processes and pools between the arid zone (a) and semiarid zone (b). The mean pool sizes (g N m^{-2}) of each soil N pool based on the bulk soil density of top 10 cm were present in the brackets. It should be noted that during both nitrification and denitrification, N trace gases NO and N_2O can be produced and escape the system ("leaky pipe" model (Firestone and Davidson, 1989), not shown in the figure), affecting both NH_4^+ and NO_3^- concentrations and their $\delta^{15}N$ values.

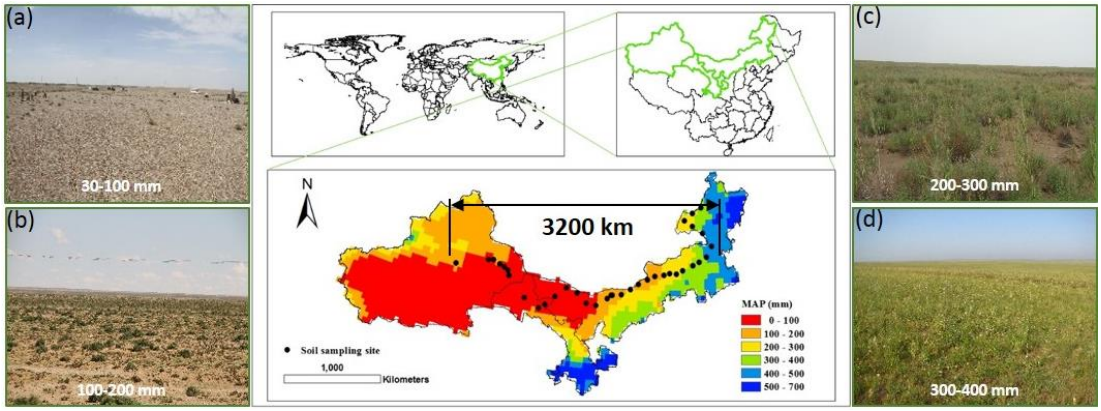
(a)
30-100 mm
(b)
100-200 mm
N
3200 km
Soil sampling site
1,000
Kilometers
MAP (mm)
0 - 100
100 - 200
200 - 300
300 - 400
400 - 500
500 - 700
(c)
200-300 mm
(d)
300-400 mm

640 **Figure 1**

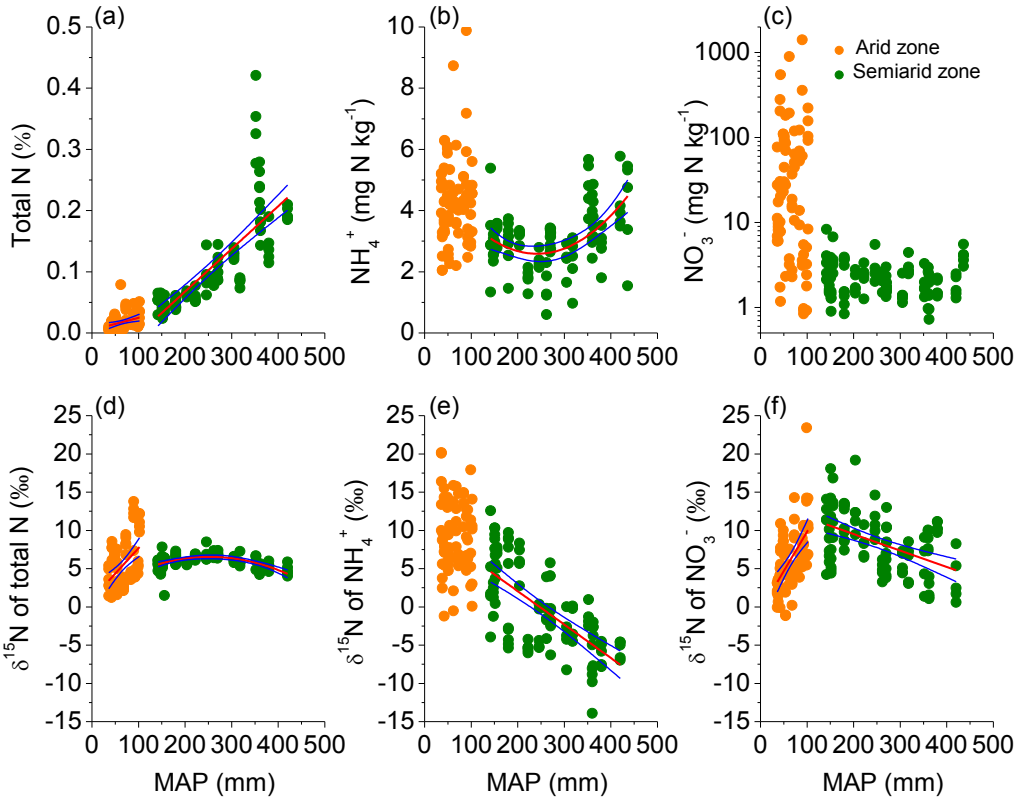
(a)
(b)
(c)
(d)
(e)
(f)
Total N (%)
NH4+ (mg N kg-1)
NO3- (mg N kg-1)
δ15N of total N (‰)
δ15N of NH4+ (‰)
δ15N of NO3- (‰)
MAP (mm)
Arid zone
Semiarid zone

Figure 2

645

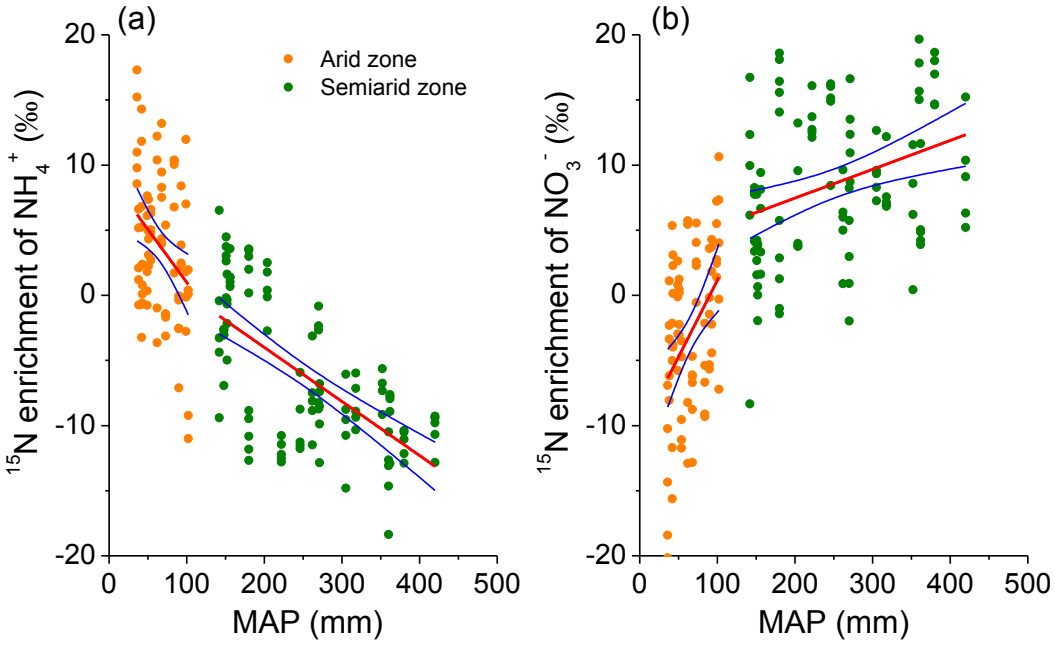
(a)
Arid zone
Semiarid zone
^{15}N enrichment of NH_4^+ (‰)
MAP (mm)
(b)
^{15}N enrichment of NO_3^- (‰)
MAP (mm)

Figure 3

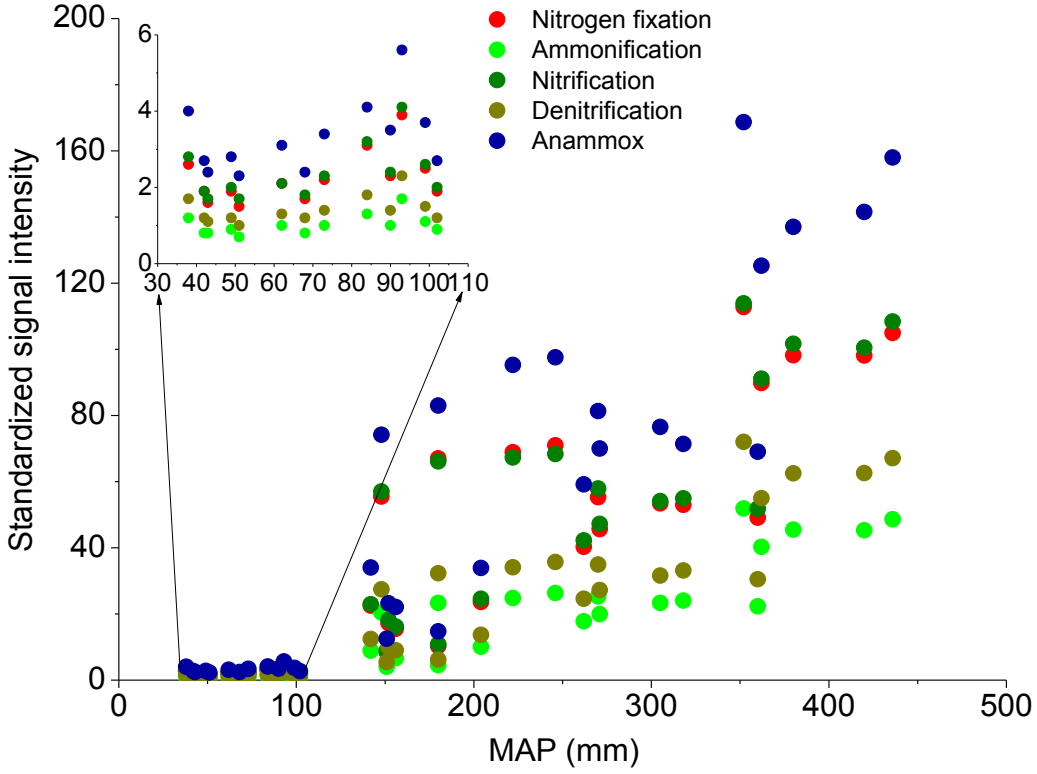
Nitrogen fixation
Ammonification
Nitrification
Denitrification
Anammox
Standardized signal intensity
MAP (mm)
0
40
80
120
160
200
0
100
200
300
400
500
0
2
4
6
30
40
50
60
70
80
90
100
110

650 **Figure 4**

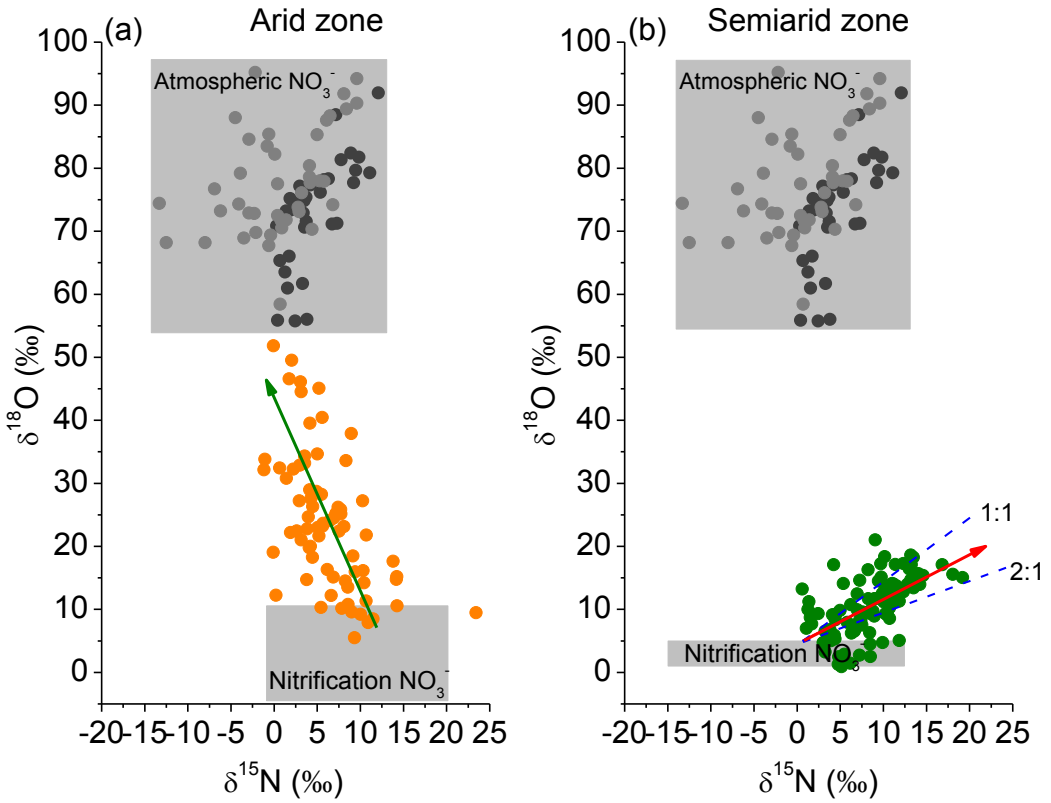
(a)
Arid zone
Atmospheric NO3-
Nitrification NO3-
δ18O (‰)
δ15N (‰)
(b)
Semiarid zone
Atmospheric NO3-
Nitrification NO3-
1:1
2:1
δ18O (‰)
δ15N (‰)

Figure 5

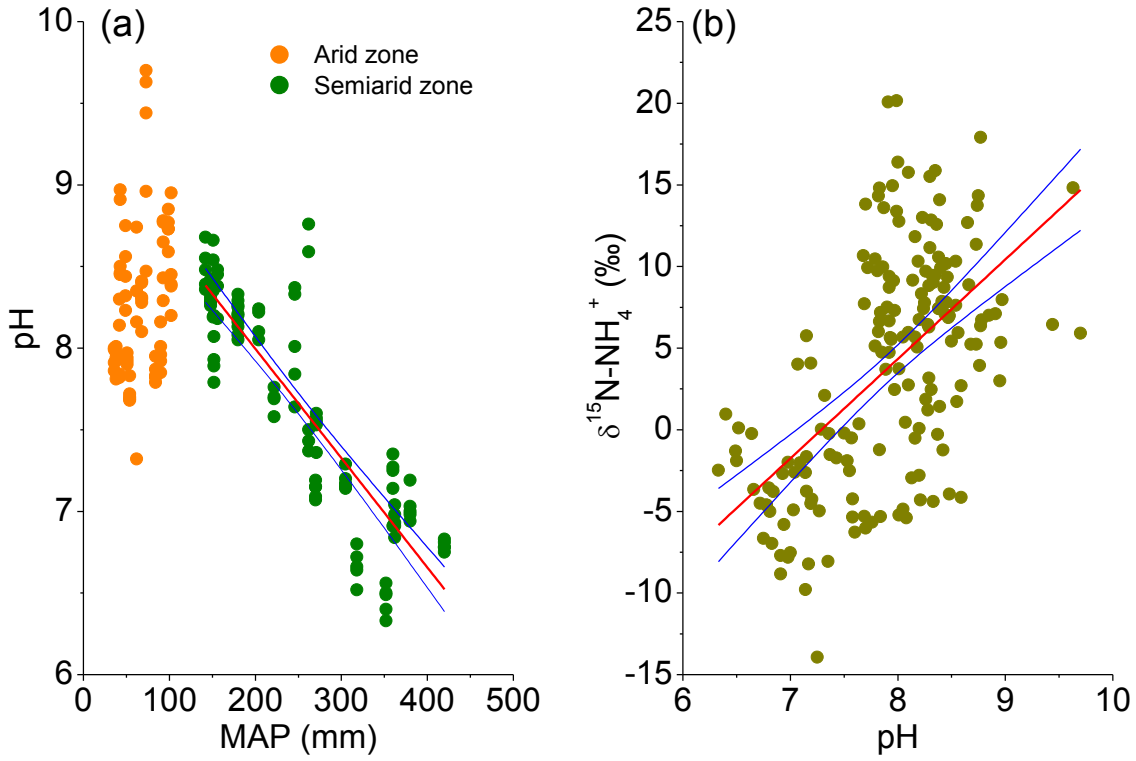
(a)
Arid zone
Semiarid zone
pH
MAP (mm)
10
9
8
7
6
0
100
200
300
400
500
(b)
$\delta^{15}N\text{-}NH_4^+$ (‰)
pH
25
20
15
10
5
0
-5
-10
-15
6
7
8
9
10

Figure 6

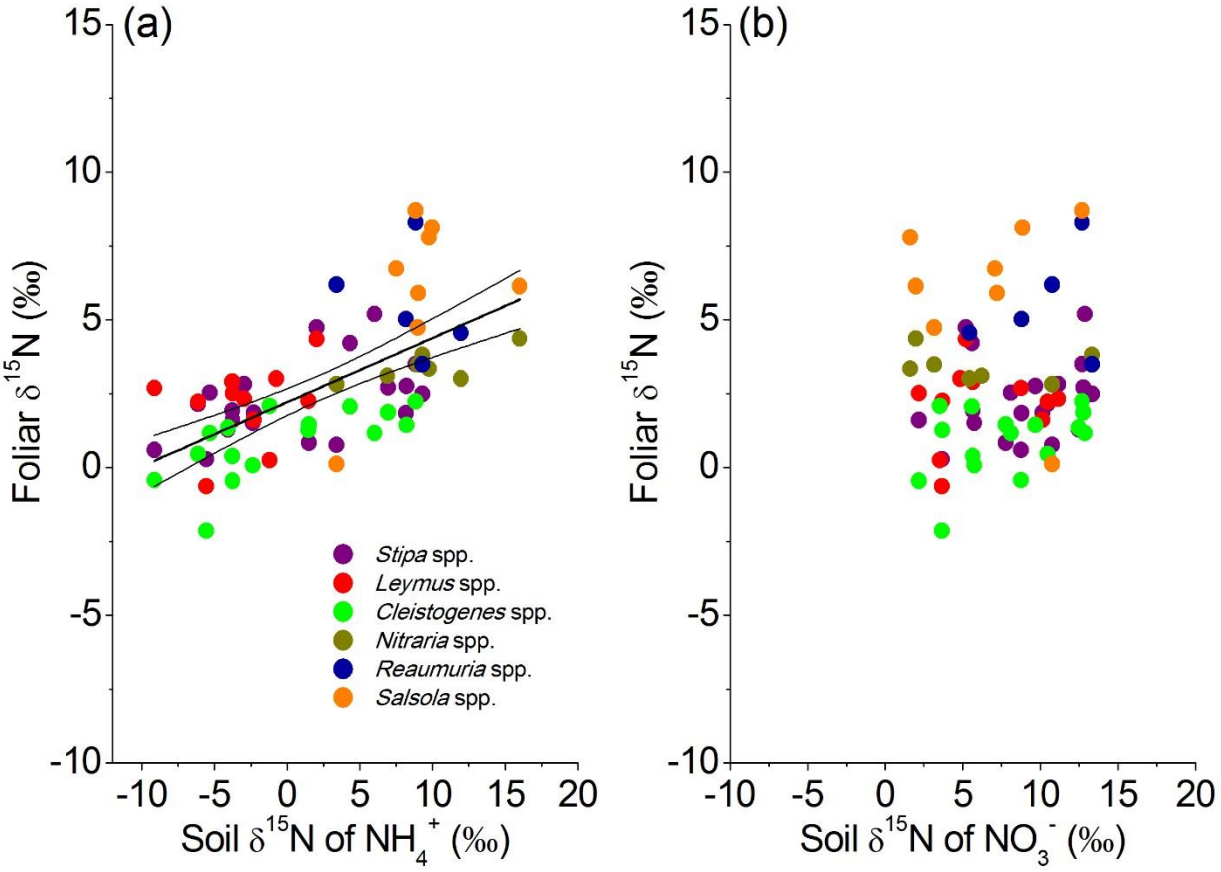
(a)
(b)
Foliar δ15N (‰)
Soil δ15N of NH4+ (‰)
Soil δ15N of NO3- (‰)
Stipa spp.
Leymus spp.
Cleistogenes spp.
Nitraria spp.
Reaumuria spp.
Salsola spp.

Figure 7

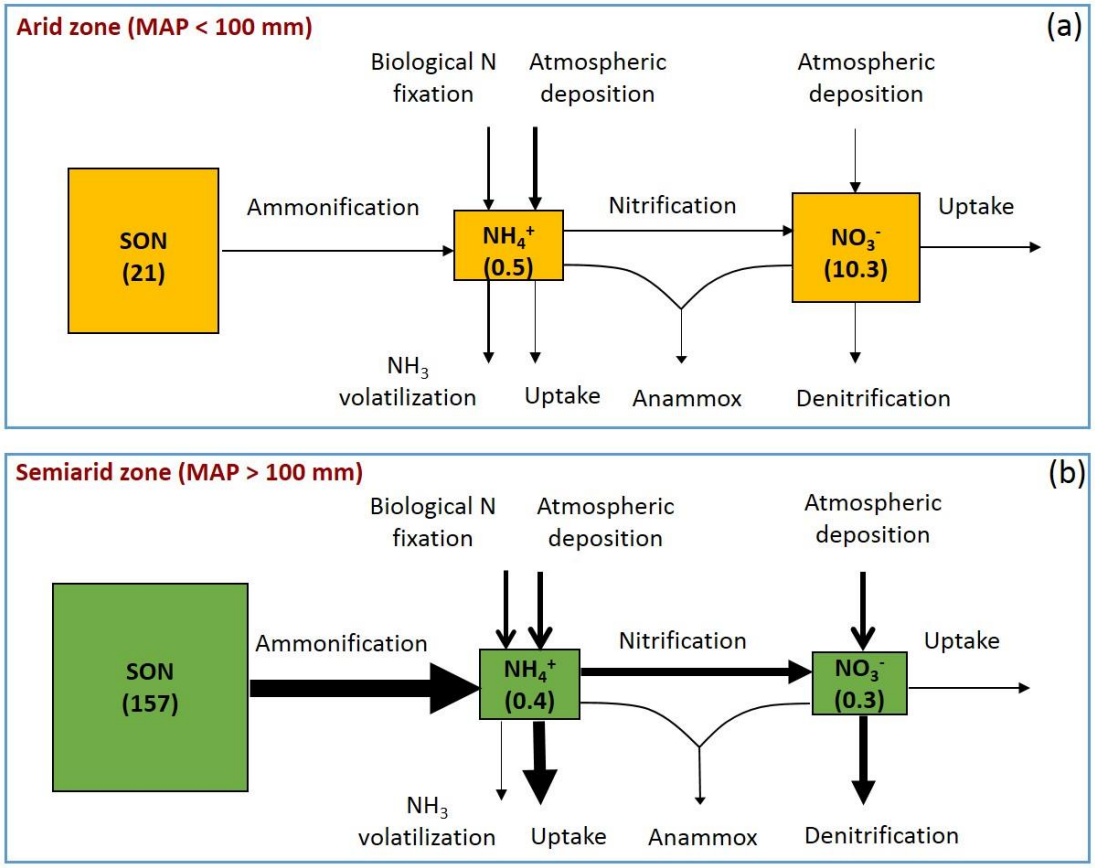
Arid zone (MAP < 100 mm)
(a)
Biological N fixation
Atmospheric deposition
Atmospheric deposition
SON (21)
Ammonification
NH4+ (0.5)
Nitrification
NO3- (10.3)
Uptake
NH3 volatilization
Uptake
Anammox
Denitrification
Semiarid zone (MAP > 100 mm)
(b)
Biological N fixation
Atmospheric deposition
Atmospheric deposition
SON (157)
Ammonification
NH4+ (0.4)
Nitrification
NO3- (0.3)
Uptake
NH3 volatilization
Uptake
Anammox
Denitrification

Figure 8

665